Computational Singular Perturbation with Non-Parametric Tabulation of Slow Manifolds for Time Integration of Stiff Chemical Kinetics

Bert Debusschere*, Youssef Marzouk†, Habib Najm*, Dimitris Goussis‡, Mauro Valorani§
*Sandia National Laboratories, Livermore, CA, USA
†Massachusetts Institute of Technology, Cambridge, MA, USA
‡National Technical University of Athens, Athens, Greece
§Sapienza University, Rome, Italy
bjdebus@sandia.gov

***Abstract*— This paper presents advances in Computational Singular Perturbation (CSP)-based time integration approaches for stiff chemical systems. By filtering fast time scales from the reaction system, CSP enables the use of explicit time integrators. For further efficiency improvements, relevant CSP quantities are re-used via non-parametric tabulation of CSP information along the slow manifolds. This paper outlines the method and shows that it is competitive with implicit solvers for the simulation of CH_4– air ignition.**

I. Introduction

The dynamics of chemical systems exhibit a wide range of time scales, with associated stiffness of the governing equations. This stiffness, and the significant complexity of chemical kinetic models, both lead to substantial challenges with the computation of chemical systems. Chemical model simplification and reduction strategies typically target these challenges by reducing the number of reactions and/or species in the model, with associated reduction in model complexity. When done properly, this strategy also reduces the system stiffness. Alternatively, the Computational Singular Perturbation (CSP)-based time integration construction of [1] uses CSP analysis to project out the fast time scales from the detailed chemical source term, thereby rendering the equations non-stiff. The promise of this approach is that explicit time integrators can be used for large-time step integration of the resulting non-stiff source terms, with associated computational speedup as compared to implicit time integration of the non-filtered detailed source term. Further, this can very well eliminate the need for operator-split time integration of reaction-diffusion source terms. Moreover, by tailoring the projection operators to the local chemical state, optimized adaptive strategies can be implemented.

The key challenge with this time integration approach, however, is the large computational cost of constructing at each time step the required CSP projection matrices, involving expensive eigenvalue solves. This computational cost can be mitigated by adaptively storing and reusing the required CSP quantities. We have explored the utility of tabulation of CSP quantities and their reuse for time integration in earlier works on elementary model problems [2], [3]. In the current work, we pursue tabulation using kd-trees [4] to efficiently store the CSP information along the slow manifolds in the chemical configuration space, without requiring *a priori* partitioning of this space. A key difference with other tabulation schemes such as ISAT [5] and PRISM [6] is that the CSP tabulation approach does not replace the time integration process, but provides the information to remove the stiffness from the chemical source term such that a more efficient explicit time integration is possible. This *explicit* and large-time step integration cost is not expected to be significant, however, and is offset by the fact that the CSP information can be tabulated in a reduced-dimensional space, resulting in substantially smaller storage and table lookup costs, especially for mechanisms with a large number of species, i.e. complex fuels.

II. CSP Integrator

Consider the chemical system described by $\frac{\mathrm{d}\boldsymbol{y}}{\mathrm{d}t} = \boldsymbol{g}(\boldsymbol{y})$, where $\boldsymbol{y} \in \mathbb{R}^N$, and $\boldsymbol{g}(\boldsymbol{y})$ is the chemical source term. The CSP basis vectors $\{\boldsymbol{a}_k\}_{k=1}^N$ and covectors $\{\boldsymbol{b}^k\}_{k=1}^N$, all in $\mathbb{R}^N$, enable the decoupling of the fast and slow processes, and the identification of low dimensional slow invariant manifolds (SIMs) [7]. Thus, we have

$$\frac{\mathrm{d}\boldsymbol{y}}{\mathrm{d}t} = \boldsymbol{g} = \boldsymbol{g}_{\mathrm{fast}} + \boldsymbol{g}_{\mathrm{slow}} \quad (1)$$

$$= \boldsymbol{a}_1 f^1 + \boldsymbol{a}_2 f^2 + \cdots + \boldsymbol{a}_N f^N \quad (2)$$

where $f^i = \boldsymbol{b}^i \cdot \boldsymbol{g}$, for $i = 1, 2, \ldots, N$. After relaxation of fast transients, with M fast modes,

$$\boldsymbol{g}_{\mathrm{fast}} = \sum_{r=1}^{M} \boldsymbol{a}_r f^r \approx 0 \quad (3)$$

$$\boldsymbol{g}_{\mathrm{slow}} = \sum_{s=M+1}^{N} \boldsymbol{a}_s f^s = (I - \sum_{r=1}^{M} \boldsymbol{a}_r \boldsymbol{b}^r)\boldsymbol{g} = \boldsymbol{P}\boldsymbol{g} \quad (4)$$

The number of fast modes M is obtained from:

$$\left| \tau_{M+1} \left(\sum_{r=1}^{M} \boldsymbol{a}_r^i f^r \right) \right| < \epsilon^i, \quad \text{with} \quad \epsilon^i = \epsilon_r |y^i| + \epsilon_a \quad (5)$$

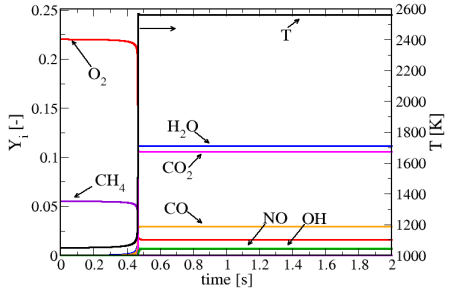

Fig. 1. Mass fractions of various species as well as temperature, in an igniting stoichiometric CH_4–air system.

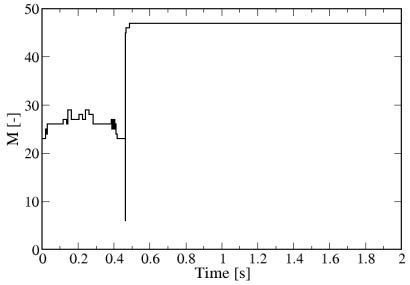

Fig. 2. The number of fast modes M determined by CSP for the trajectory in Fig. 1.

and τ_{M+1} is the time scale associated with mode $M+1$, the fastest of the slow modes, which drives the dynamics of $\boldsymbol{y}$ at this point.

The CSP integrator [1] first integrates the slow dynamics of the system, followed by a homogeneous correction (HC) to account for processes on the fast time scales:

$$\tilde{\boldsymbol{y}}(t+\Delta t) = \boldsymbol{y}(t) + \int_t^{t+\Delta t} \boldsymbol{P}\boldsymbol{g}\,\mathrm{d}t' \quad (6)$$

$$\boldsymbol{y}(t+\Delta t) = \tilde{\boldsymbol{y}}(t+\Delta t) - \sum_{m,n=1}^{M} \boldsymbol{a}_m \tau_n^m|_t \hat{f}^n \quad (7)$$

$$\hat{f}^n = \boldsymbol{b}^n \cdot \boldsymbol{g}[\tilde{\boldsymbol{y}}(t+\Delta t)] \quad (8)$$

where τ_n^m is the inverse of λ_n^m, both in $\mathbb{R}^{N\times N}$, given by

$$\lambda_n^m = \left(\frac{\mathrm{d}\boldsymbol{b}^m}{\mathrm{d}t} + \boldsymbol{b}^m \boldsymbol{J}\right)\boldsymbol{a}_n \quad (9)$$

and $\boldsymbol{J}$ is the Jacobian of $\boldsymbol{g}$. The matrix τ_n^m is diagonal with entries the time scales $\{\tau_k\}_{k=1}^N$ when the CSP basis vectors are chosen to be the eigenvectors of $\boldsymbol{J}$ and the curvature of the SIM is neglected, *i.e.* $\mathrm{d}\boldsymbol{b}^m/\mathrm{d}t = 0$.

For both accuracy and stability, the explicit time integration procedure can take time steps on the order of the driving time scale τ_{M+1}: $\Delta t = \alpha\,\tau_{M+1}$, with the time step factor $\alpha : 0 < \alpha \leq 1$ determining the trade-off between accuracy and efficiency.

We further note that the CSP pointer [8] allows the identification of *CSP radicals*, namely those species most associated with the fast modes. The M CSP radicals are the optimal candidates to be determined from the constraints Eq. (3) associated with the slow manifold, and are thus slaved to the $N-M$ remaining species, which we term *non-radicals*. An important consequence of this is that the CSP quantities along a slow manifold are only a function of the $N-M$ non-radicals, allowing tabulation in a reduced-dimensional space.

III. CSP with Tabulation: CH_4–Air Ignition

Consider the constant pressure ignition of a homogeneous CH_4–air mixture, modeled with the GRI 3.0 mechanism [9], which includes 325 reversible reactions and 53 species, for a chemical state space dimension of $N = 54$ (including T). For a stoichiometric mixture with an initial temperature of 1050 K, the evolution of the temperature T and the main species mass fractions Y_i is shown in Fig. 1, based on computations using the implicit CVODE [10] time integrator. For this reaction mechanism, the number of fast modes M, as determined with CSP, is shown in Fig. 2. Initially, the number of fast modes varies between 23 and 29. During the fast ignition transient, M drops down to 6 for a very short time, and then rapidly evolves to a steady state with 47 fast modes. This large number of fast modes during the bulk of the simulation offers tremendous potential for stiffness reduction and corresponding computational speed-ups.

To test the performance and accuracy of CSP with tabulation, a number of tables were constructed using CSP information from design points extracted from a set of detailed simulations. Those simulations used an initial temperature of 1050 K, and an initial equivalence ratio sampled from a uniform grid on $0.95 \leq \phi \leq 1.05$. The results of 5 tables are illustrated here, named T_CH_4.nX.fY, where X is the number of samples from the range of initial equivalence ratios, and Y controls the number of design points extracted from each detailed simulation. The number of design points in each table is approximately proportional to X and inversely proportional to Y, with the smallest table T_CH_4.n50.f1e-2 containing 14985 states on 60 different manifolds, and the largest table T_CH_4.n50.f1e-3 containing 125948 states on 69 manifolds. Given the high dimensionality of the chemical configuration space, we use kd-trees [4] with dimensions $N-M$ to efficiently store the CSP information without requiring *a priori* partitioning of this space. For retrieval of CSP information, a nearest-neighbor lookup is performed in each tabulated manifold, and the CSP integrator uses the CSP information of the tabulated state nearest to the current state, if this tabulated state is within a threshold distance d_{Max}. If no satisfactory tabulated state can be found, a full CSP analysis is performed instead.

For all cases studied, the temperature and species profiles obtained from detailed chemistry, CSP, or CSP with tabulation were visually indistinguishable (not shown). A quantitative analysis of the predicted ignition times (defined as the time at which the temperature rise reaches half its equilibrium value) showed relative errors (compared to detailed chemistry simulation) on the order of 10^{-6} for CSP, and relative errors on the order of 10^{-5} to 10^{-4} for CSP with tabulation (not shown). A more sensitive measure of deviations between the simulated profiles is an RMS distance, averaged over T and all species, over

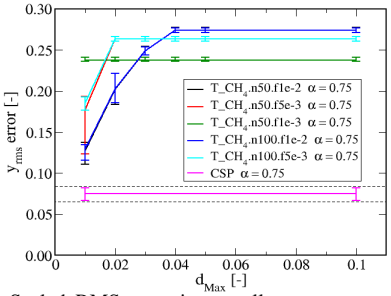

Fig. 3. Scaled RMS error in overall system state from CSP with and without tabulation compared to detailed chemistry simulations. The dashed lines indicate the errors for regular CSP. The errors are averaged over 100 simulations with randomly sampled initial conditions, with "error bars" indicating the 5% and 95% quantiles. Time step factor $\alpha = 0.75$.

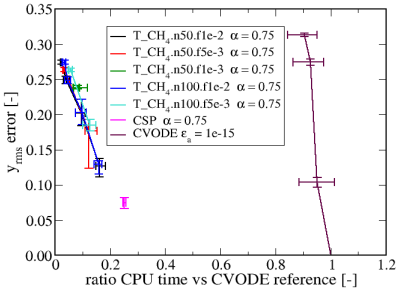

Fig. 4. RMS error versus relative CPU time for CH_4–air ignition simulated with detailed chemistry, or with CSP with and without tabulation. The reference is a detailed chemistry simulation with tight tolerances.

all time points, with each profile scaled to range between 0 and 1, in order to give trace species equal importance as other species. As shown in Fig. 3 this scaled RMS error is nearly constant for large values of d_{Max} in the table look-up, and generally gets smaller for larger tables. Below a given value of d_{Max}, the observed RMS error decreases towards the error observed with CSP, reflecting the fact that the table look-up is less and less successful for smaller d_{Max} values, and a CSP analysis is increasingly used instead.

In terms of overall efficiency, Fig. 4 compares the RMS error versus CPU time for the various simulation methods. The CPU time is expressed as a ratio of the observed CPU time versus the CPU time required to simulate the same cases by integrating the detailed kinetic mechanism with CVODE using tight tolerances (relative tolerance of 10^{-8}, absolute tolerance of 10^{-15}) on the desired accuracy. These same high accuracy CVODE simulations are also the reference in the computation of the RMS error of the various simulation approaches. Note that the CVODE solver was made to reset its work arrays after each time step, in order to emulate the way the CVODE solver would be used in a reacting flow simulation, with operator splitting between the transport and chemistry terms. Each point in the curves for CSP with tabulation corresponds to a different setting of d_{Max} (with smaller d_{Max} settings generally corresponding to smaller RMS errors, per Fig. 3). Varying the relative tolerance in CVODE from 10^{-8} to 10^{-5} (with the absolute tolerance kept at 10^{-15}) for detailed chemistry simulations results in a strong drop in accuracy for modest CPU time savings. The graph shows that the CSP integrator by itself is on average 4 times faster than direct integration of the detailed kinetics with CVODE for the cases under consideration. Using tabulation, the simulations are up to 40 times faster than CVODE, for comparable errors. These results cleary show the potential of CSP with tabulation to speed up the simulation of complex kinetics. More results are discussed in [11].

IV. Conclusions

This paper demonstrated the use of an adaptive non-parametric tabulation approach to allow efficient reuse of CSP information in order to improve the computational efficiency of the CSP integrator. The approach relies on kd-trees to store CSP information in a reduced-dimensional space. When applied to the ignition of homogeneous CH_4–air mixtures, modeled with the GRI3.0 kinetic mechanism, tabulation was shown to improve the performance of the CSP integrator with a factor of 10, resulting in an overall factor of 40 speed-up compared to direct integration of the detailed reaction mechanism with CVODE while maintaining good overall accuracy.

Acknowledgment

This work was supported by the US Department of Energy, Office of Basic Energy Sciences, SciDAC Computational Chemistry program. Sandia National Laboratories is a multi-program laboratory operated by Sandia Corporation, a wholly owned subsidiary of Lockheed Martin Corporation, for the U.S. Department of Energy's National Nuclear Security Administration under contract DE-AC04-94AL85000. M.V. acknowledges the support of the Italian Ministry of University and Research.

References

[1] Valorani, M., and Goussis, D.A., *J. Comp. Phys.*, 169:44–79 (2001).
[2] Lee, J.C., Najm, H.N., Lefantzi, S., Ray, J., Frenklach, M., Valorani, M., and Goussis, D., *Comb. Theory and Model.*, 11(1):73–102 (2007).
[3] Lee, J.C., Najm, H.N., Lefantzi, S., Ray, J., and Goussis, D.A., in *Computational Fluid and Solid Mechanics* (K. Bathe, Ed., Elsevier Science, pp. 717–720, (2005).
[4] Arya, S., Mount, D. M., Netanyahu, N. S., Silverman, R., and Wu, A. Y., *J. ACM*, 45(6):891–923 (1998).
[5] Pope, S.B., *Comb. Theory and Model.*, 1:41–63 (1997).
[6] Tonse, S. R., Moriarty, N.W., Brown, N.J., and Frenklach, M., *Israel Journal of Chemistry*, 39:97–106 (1999).
[7] Lam, S.H., and Goussis, D.A., *Proc. Comb. Inst.*, 22:931–941 (1988).
[8] Valorani, M., Najm, H.N., and Goussis, D., *Comb. and Flame*, 134(1-2):35–53 (2003).
[9] Smith, G.P., Golden, D.M., Frenklach, M., Moriarty, N.W., Eiteneer, B., Goldenberg, M., Bowman, C.T., Hanson, R.K., Song, S., Jr., W.C. Gardiner, Lissianski, V.V., and Zhiwei, Q., *www.me.berkeley.edu/gri_mech/*.
[10] Brown, P.N., Byrne, G.D., and Hindmarsh, A.C., *SIAM J. Sci. Stat. Comput.*, 10:1038–1051 (1989).
[11] Debusschere, B.J., Marzouk, Y.M., Najm, H.N., Rhoads, B., Goussis, D.A., and Valorani, M., *Comb. Theory and Model.*, under revision (2010).